

Evidences of accelerating the increase in the concentration of methane in the atmosphere after 2014: satellite data for the Arctic.

L.N. Yurganov¹, I. Leifer², S. Vadakkepuliambatta³

¹ *University of Maryland Baltimore County, Baltimore, 21250, USA*

E-mail: yurganov@umbc.edu

² *Bubbleology Research International, Santa Barbara, 93106, USA*

³ *Centre for Arctic Gas Hydrate, Environment and Climate, Department of Geosciences, UiT- The Arctic University of Norway, Tromsø, 9037, Norway.*

English translation.

To be published in the “*Current problems in remote sensing of the Earth from space*”, v. 14, No ?, 2017 (in Russian), <http://jr.rse.cosmos.ru/?lang=eng>

European orbital IASI/MetOP-A interferometer TIR radiation data were processed by NOAA for methane profiles and uploaded in a publicly accessible archive. Satellite measurements for the middle and high latitudes of the Northern Hemisphere reveal a concentration growth rate of 4-9 ppbv/year in 2010-2013 and up to 12-17 ppbv/year in the 2015-2016. Global estimates based on surface measurements of NOAA at coastal stations for the same periods show an increase from 5-6 ppbv/year after 2007 to 9-12 ppbv/year last two years. Satellite data allow analyzing the methane concentration both over land and over the Arctic seas in the absence of near-surface temperature inversions. The results of remote measurements are compared with direct aircraft measurements in summer-autumn Alaska during the CARVE experiment. The maximum anomalies of methane (in comparison with a relatively clean area between Scandinavia and Iceland) were observed in November-December over the sea surface along the coasts of Norway, Novaya Zemlya, Svalbard and other regions of the Arctic. Anomalies were insignificant in summer. Over the years, the winter anomalies (contrasts) grew: the maximum rate was recorded for the area to the west of Novaya Zemlya (9.4 ± 3.7) ppbv/year. Above Alaska, the anomaly of methane concentration in summer, when the microbiological sources are active, increased at a rate (2.6 ± 1.0) ppbv/year. The locations of the maxima of the anomaly around Svalbard correspond to the observed methane seeps from the seabed and the predicted regions of dissociation of methane hydrates. The observed methane acceleration during the last two years does not necessarily indicate a long-term tendency: 2015-2016 was a strong El-Niño period.

Keywords: IASI, remote sensing, atmospheric methane, methane hydrates

Introduction

Methane (CH₄), as a greenhouse gas, is the second important after the carbon dioxide. The mixing ratio of methane in the atmosphere in 1983 -1991 has been increasing at a rate of 10-15 ppbv (parts per billion by volume) per year, then the growth slowed down and in 2000-2006 its mixing ratio was almost stable. In 2007 - 2014 the rate of methane growth rate was ~ 5-6 ppbv per year (Saunio et al., 2016). Dlugokencky et al. (2009) proposed several mechanisms responsible for the observed pattern of methane variations, but there is still no consensus on this (Saunio et al., 2016). The

network of NOAA stations allows monitoring of surface methane with high accuracy, but stations are unevenly distributed (Dlugokencky et al., 2009). For example, systematic data on methane concentrations in the air over the Arctic Ocean are not available, only campaign-based measurements from ships and aircrafts are known mainly in summer seasons (Shakhova et al., 2010, Myhre et al., 2016). Plumes of methane bubbles in the ocean column, including those from methane hydrates, are reliably detected by sonars (Veloso et al., 2015, Obzhirov, Telegin and Bologbank, 2015). It is still unclear, however, how big is the flow of methane through the sea/air interface into the atmosphere. In the summer, for example, it is very small (Myhre et al., 2016), but in the autumn-winter period it has not been adequately studied. The current warming of the Arctic can cause rapid destruction of methane hydrates and a significant increase in its concentration in the atmosphere with subsequent adverse effects on the climate (AMAP, 2015).

Remote satellite sounding, based on spectrometers measuring the Earth's own radiation, rather than reflected sunlight, is a promising method for studying atmospheric methane in the Arctic. Yurganov, Leifer and Lund-Myhre (2016) (hereinafter referred to as YLL-1) demonstrated the possibility of year-round measurements, including the polar night, of methane over the surface of the Arctic and subarctic seas using Thermal IR (TIR) satellite spectrometers. Yurganov and Leifer (2016a) (hereinafter referred to as YL-2) determined the areas of the Arctic Ocean with maximum methane emissions in the autumn-winter period: along the coasts of Norway, Novaya Zemlya and Svalbard, as well as the Sea of Okhotsk. Yurganov and Leifer (2016b) (hereinafter referred to as YL-3) drew attention to a sharp increase in methane mixing ratio over the Okhotsk Sea in the winter of 2015/2016 compared with previous years.

In this paper, an acceleration of methane mixing ratio growth in 2015-2016 compared with the previous 5-year period in the middle and high latitudinal belts of the northern hemisphere is noted. Mixing ratios of methane over some areas of the Arctic Ocean increased at a rate higher than in the North Atlantic. The degree of Arctic influence on global methane, however, is still unclear and requires a separate consideration.

Method validation

The data of the European satellite interferometer IASI/MetOP-A on mixing ratios of methane by volume were obtained by the method described by Xiong et al. (2013) and taken from the NOAA archive (<https://www.nsof.class.noaa.gov/saa/products/welcome>). YLL-1 defined thermal contrast (ThC) as a temperature difference between the surface and the height of 4 km. It was found that for $\text{ThC} < 10^\circ \text{C}$ the instrument sensitivity to the lower troposphere drops down. For this reason, all the data for $\text{ThC} < 10^\circ \text{C}$ were excluded from consideration. The remaining methane profiles were averaged separately for altitudes of 0-4 km and 4-13 km.

Xiong et al. (2013) investigated the reliability of methane measurements by the IASI instrument and demonstrated its high sensitivity to methane in the middle and high troposphere. In the same work, a conclusion was made about the reduced sensitivity of the method to the lower layers of the atmosphere (below 4 km of altitude). It should be noted, however, that Xiong et al. (2013) used for validation mainly the results of aircraft measurements in the cleanest areas of the Pacific Ocean.

Meanwhile, sources of methane are located on the land surface, they may increase its mixing ratios up to 3-4 ppmv (parts per million by volume), i.e. doubling its background (Leifer et al., 2017). At such high mixing ratios the instrument can be capable of examining the lower troposphere even with reduced sensitivity. For this reason, an additional validation is required in the presence of surface methane sources.

YLL-1 compared the mixing ratios of methane measured by IASI over an open water surface near the Svalbard, where deposits of methane hydrates were discovered (Myhre et al., 2016), with local measurements at the coastal station Zepellin located at the elevation of 474 m (Fisher et al., 2011, updated until the end of 2014). A good agreement for monthly values was demonstrated. Daily mixing ratios, however, disagree. The authors explained this effect by the location of the Zepellin station near the upper limit of the tropospheric boundary layer and corresponding high variability of methane mixing ratios there.

A publication of full-scale aircraft measurements of methane in the warm period of the year (May - November) from 2012 to 2014 over Alaska during the experiment Carbon in Arctic Reservoirs Vulnerability Experiment (CARVE, Chang et al., 2014; Miller et al., 2016; Budney et al., 2016; https://daac.ornl.gov/cgi-bin/Dsviewer.pl?ds_id=1402) allowed us to implement more reliable validation of satellite measurements for the lower troposphere. The greatest number of flights conducted over the southwestern part of Alaska lowland consisting Yukon valley and Seward Peninsula, in triangle with vertices at [(64° N, 150° W), (59° N, 165° W), (67° N, 168° W)]. The monthly methane mixing ratios in the 0-4 km layer measured by the IASI over the specified area, with standard deviation of 15-20 ppbv and a total of 81,591 points, were compared with the readings of the Picarro laser analyzer in the 0-1 km height range with an error of 0.3 ppbv and the total number of points 106,490 (*Fig.1*). A significant spread of the average monthly results (correlation coefficient $R=0.65$) can be explained by the horizontal and vertical inhomogeneities in the distribution of methane values. The slope of the regression line obtained by the least squares method is 0.69 (the upper and lower confidence intervals with a reliability of 95%, calculated according to Chatterjee and Hadi (1986), were 0.90 and 0.47, respectively), characterizes the sensitivity of the remote sensing method to the methane variations in the lower layer of the troposphere for specific summer conditions in Alaska. In practice, this means that the remote method underestimates the real variations by about 30% on average. Unfortunately, there are only a very few direct airborne methane measurements over the Arctic Ocean surface, especially in November-December. Therefore, a decisive verification of satellite measurements over the Arctic ocean is still pending.

Results of satellite methane measurements

As have been already noted, the data in the 4-13 km layer are found the most reliable (Xiong et al., 2013). The red dots in Figure 2 are the 10-days IASI methane 4-13 km averages for the latitudinal belt 45° N- 85° N and black triangles are corresponding data for the 60° N – 85° N. The red and black lines are moving averages over 3 years. In both latitudinal belts the acceleration of methane increase is detected beginning with early 2014. For comparison, the monthly surface mixing ratios

of methane averaged over all stations of the NOAA network (Dlugokencky et al., 2009) updated until December 2016 (https://www.esrl.noaa.gov/gmd/ccgg/trends_ch4/) are shown in blue. The year-to-year changes in methane (the differences between mixing ratios of the designated year and the previous one) are listed in *Table.1*. In 2010-2013 satellite measurements to the North of 45° N undergo the rate of mixing ratio increase 4-9 ppbv/year. In 2015 and 2016 mixing ratios increased by 12 and 17 ppbv/year, respectively. Global estimates based on near-surface measurements of NOAA at coastal stations for the same periods show an increase from ~5 ppbv/year to 9-12 ppbv/year. The difference in growth rate between the Arctic (to the North of 60° N) and a portion of the northern hemisphere to the North of 60° N (*Fig. 2, Tab. 1*) practically absent. The third line of *Table. 1* shows similar data for North Atlantic polygon taken for comparison with the Arctic (see below).

Table 1. The rates of increase of methane mixing ratio according to IASI (4-13 km altitude) and the surface of the Earth at NOAA network, ppbv/year

<i>Years</i>	<i>2011</i>	<i>2012</i>	<i>2013</i>	<i>2014</i>	<i>2015</i>	<i>2016</i>
IASI, 45 ° -85 ° N	3.7	7.7	7.8	9.7	11.6	16.7
IASI, 60 ° -85 ° N	3.1	7.2	9.9	11.4	9.2	18.8
IASI, N. Atlantic	2.8	6.3	6.0	8.0	5.9	19.5
NOAA, globally	4.3	5.2	5.1	9.2	11.5	9.1

Let us consider how the methane mixing ratio in the lower troposphere has been changing over certain areas of the Arctic in more detail. To separate the contribution of Arctic sources to atmospheric methane from methane transfer from lower latitudes, it is necessary to calculate the anomaly of methane; the North Atlantic between Scandinavia and Iceland (*Fig. 3, Tab. 1*) has been selected as a reference. The mixing ratios of methane over the reference area were subtracted from all data. Maps in *Fig. 3, a* and *b*, illustrate changes in contrast in November-December methane mixing ratio between source areas and the reference area. Five Arctic areas with an increased anomaly have been selected for further analysis: off the coast of Norway, Greenland, Novaya Zemlya and Svalbard (in the latter case, the Western and Eastern parts separately), as well as a sub-Arctic Sea of Okhotsk.

A year-to-year growth of methane anomalies in the autumn-winter period is shown by the example of the maritime areas to the West and East of Spitsbergen (*Fig. 4*). Regression analysis (*Fig. 5* and *Table 2*) is carried out to quantify the anomalies of growth rates in selected portions of the surface of the Arctic seas and Okhotsk. The boundaries of the three selected areas are shown in *Fig. 3*; vertex coordinates of the Greenland quadrangle are [(75° N, 61° W), (75° N, 53° W), (57° N, 43° W), (57° N, 51° W)]. In the range of latitude 78° N - 80° N the methane anomaly East of Spitsbergen grew faster than west of Spitsbergen (6.2 versus 4.8 ppbv/year). The maximum growth rate was observed to the West of Novaya Zemlya: 9.4 ppbv/year.

A slower growth of the methane anomaly during the maximum emission period in July-September was found in Alaska: 2.6 ppbv/year (for the boundaries of the selected region in Alaska see above). Note that the lower limits of the confidence intervals with a reliability of 95% for the slope of the linear regression line in all cases, including Alaska, were positive.

Table 2. The slope of the linear linear mean square regression for the methane anomaly over different sections in the Arctic ocean (0-4 km) in November-December and the correlation coefficients.

Area	Slope, ppbv/year	UBCI, ppbv/year	LBCI, ppbv/year	Correlation coefficient
North of Norway	3.79	5.33	2.25	0.87
West of Spitsbergen	4.80	7.42	2.18	0.77
East of Svalbard	6.24	8.47	4.01	0.90
West of Novaya Zemlya	9.43	13.18	5.68	0.88
West of Greenland	7.06	11.64	2.48	0.68
Sea of Okhotsk	7.62	12.63	2.61	0.67
Alaska (July - September)	2.56	3.55	1.57	0.88

UBCI: upper bound of confidence interval for slope, LBCI: lower bound of confidence interval (reliability 95%).

Discussion

The mixing ratio of methane in the atmosphere experiences seasonal variations and an interannual trend. Seasonal variations are caused by variations in the photochemical sink of methane determined by hydroxyl, which is responsible for ~83% of its global removal (Saunois et al., 2016). For this reason, the amplitude of seasonal variations in the high latitudes (*Fig. 2*) is higher than global. The interannual trend is most likely due to the growth of the global emissions of methane (Saunois et al., 2016).

The increase in the rate of methane growth in the past two years, both in the Arctic and global (NOAA network), does not necessarily indicate a long-term trend: 2015 and 2016 were characterized as the period of one of the strongest effects of El-Nino (Varotsos, Tzanis, and Sarlis, 2016). Nevertheless, the satellite data for most of the considered areas (except the Sea of Okhotsk, *Figure 5*) indicate an intensification of methane emissions from the Arctic Ocean into the atmosphere in the winter months during the entire measurement period, not only in the 2015-2016.

In the summer months, both satellite data (YLL-1, YL-3) and direct measurements in the ocean and atmosphere (Myhre et al., 2016), evidence in insignificant methane flux. A growth of emissions since early November can be explained by a break down of the stable thermal stratification in the ocean and efficient mixing of sea water (Dobrovolsky and Zalogin, 1982). If we assume that the rate of autumn-winter emission of methane from the seas of the West Arctic is proportional to its anomaly, then for seven years it has doubled.

The specific mechanism for the formation of methane in the West Arctic Ocean is not fully understood. There is an evidence of methane formation in the surface layer of the ocean in melting ice (Damm et al., 2015). However, the prevailing view is the dissociation of methane hydrates under the seabed (AMAP, 2015; Veloso et al., 2015). The area to the West of Spitsbergen has been studied most fully (Veloso et al., 2015). Satellite data confirm the presence of significant anomalies of methane mixing ratios in this region since November (YLL-1, YL-2). This paper has shown that to the East of Spitsbergen, methane anomalies grow with years even faster than to the West of it. Myhre et al., (2016) published a map of recorded methane seeps and predicted methane emissions from methane hydrates west of Spitsbergen. Using the same methodology, we calculated the positions of the potential emissions of methane areas to the East of Spitsbergen (*Fig. 6*). Satellite data are in complete agreement with the locations of expected of emissions from methane hydrates at both sides of Spitsbergen. Another well-known area rich in methane hydrates, the Sea of Okhotsk (Soloviev et al., 1982, Obzhirov, Telegin and Bologbank, 2015), also reveals high methane anomalies in 2015 and 2016. (*Fig. 5*).

The question of how much do the Arctic methane sources influence global methane requires numerical experiments on climate models (Volodin 2015) and is beyond the scope of this paper.

Acknowledgements

The authors are grateful to E. Dlugokencky (NOAA) for the opportunity to use the latest global data on methane and NASA for publishing the results of the CARVE program. The job has been accomplished thanks to a grant from NASA «Long-term Satellite Data Fusion Observations of Arctic Ice Cover and Methane as a Climate Change Feedback".

References

1. Volodin E.M. The influence of methane sources in the high latitudes of the northern hemisphere on the interhemispheric asymmetry of its concentration and on the climate // *Izv. RAS. Physics of the atmosphere and ocean*. 2015. 51. T. number 3. pp 287- 294.
2. Dobrovolskiy A. D., Zalogin B.S. Sea of the USSR. M. Izd-vo MGU. 1982. c. 96
3. Obzhirov AI, Telegin Yu.A., Boloban AV. Streams of methane and gas hydrates in the Sea of Okhotsk // Underwater Investigation and Robotics. 2015. T.19. № 1. P. 56-63.
4. VA Soloviev, G. Ginzburg, AI Obzhirov Douglas VK. Gas hydrates of the Sea of Okhotsk // *Domestic Geology*. 1994. №2. Pp. 10-17.
1. Yurganov L.N., Leifer I., Lund-Myhre C., Sezonnaya i mezhgodovaya izmenchivost' atmosfernogo metana nad moryami Severnogo Ledovitogo okeana po sputnikovym dannym (Seasonal and interannual variability of atmospheric

- methane over Arctic Ocean from satellite data), *Sovremennye problemy distantsionnogo zondirovaniya zemli iz kosmosa*, 2016, Vol. 13, No 2, pp. 107-119.
2. Yurganov L.N., Leifer I., Otsenki emissii metana ot nekotorykh arkticheskikh i priarkticheskikh rayonov po dannym orbital'nogo interferometra IASI (Estimates of methane emission rates from some Arctic and sub-Arctic areas, based on orbital interferometer IASI data), *Sovremennye problemy distantsionnogo zondirovaniya zemli iz kosmosa*, 2016, Vol. 13, No 3, pp. 173-183.
 3. Yurganov L.N., Leifer I. Anomal'nye konsentratsii atmosfernogo metana nad Okhotskim morem zimoi 2015/2016 g.g. (Abnormal concentrations of atmospheric methane over the Sea of Okhotsk during 2015/2016 winter), *Sovremennye problemy distantsionnogo zondirovaniya zemli iz kosmosa*, 2016b, Vol. 13, No 3, pp. 231-234.
 8. AMAP Assessment 2015: Methane as an Arctic climate forcer: Arctic Monitoring and Assessment Programme (AMAP). 2015. Oslo, Norway. 139 pp. ISBN - 978-82-7971-091-2.
 9. Budney JW, Chang RY-W., Commane R., Daube BC, Dayalu A., Dinardo SJ, Gottlieb EW, Karion A., Lindaas JOW, Miller CE, Miller JB, Miller S., Pender M., Pittman JV, J. Samra, Sweeney C., Wofsy SC, and Xiang B. 2016. CARVE: L2 Merged Atmospheric CO₂, CO, and CH₄ O₃ Concentrations, Alaska, 2012-2015. ORNL DAAC, Oak Ridge, Tennessee, USA. <http://dx.doi.org/10.3334/ORNLDAAC/1402>
 10. YW R. Chang., CE Miller, SJ Dinardo, Karion A., C. Sweeney, Daube BC, JM Henderson, Mountain ME, Eluszkiewicz J., Miller JB, Bruhwiler LMP, and Wofsy SC Methane emissions from Alaska in 2012 from CARVE airborne observations // Proceedings of the National Academy of Sciences of the United States of America. 2014. Vol. 111. number. 47, pp. 16694-16699.
 - eleven. Chatterjee, S., Hadi AS Influential observations, high leverage points, and outliers in linear regression // Statistical Science. 1986. Vol. 1, pp. 379-416.
 12. E. Damm, B. Rudels, U. Schauer, S. Mau, G. Dieckmann Methane in Arctic excess surface water-triggered by sea ice formation and melting // Reports Scientific. 2015. Vol. 5. 16179.
 13. EJ Dlugokencky, Bruhwiler L., White JWC, LK Emmons, Novelli PC, SA Montzka, Masarie KA, Lang Card PM, Crotwell AM, Miller JB, and Gatti LV Observational constraints on recent increases in the atmospheric CH₄ burden // Geophysical Research Letters . 2009. Vol. 36. L18803.
 14. Fisher RE, Sriskantharajah S., Lowry D. , Lanoisellé M., Fowler CMR, James RH, Hermansen O., Lund Myhre C., Stohl A., Greinert J., Nisbet-Jones PBR, Mienert J., Nisbet E. the G . Arctic methane sources: isotopic evidence for atmospheric inputs // Geophysical Research Letters. 2011. Vol. 38. L21803.
 15. Leifer I., C. Melton, Buckland KN, Clarisse L., Coheur Frash P. J., M. Gupta, Tratt DM, Leen JB, Van Damme M., Whitburn S., Yurganov L. Remote sensing and in situ measurements of methane and ammonia emissions from a megacity dairy complex: Chino, CA // Environmental Pollution. 2017. Vol. 221. pp. 37-51.
 16. Miller S., Miller C., Commane R. , Chang R.-W., Dinardo S., Henderson J., Karion A., Lindaas J., Melton J., Miller J., Sweeney C., Wofsy S. , Michalak A. The A multi-year Estimate of methane Fluxes in Alaska You CARVE from atmospheric // Observations of Global Biogeochemical Cycles. 2016. Vol. 30. pp. 1441 - 1453 .
 17. Myhre CL, Ferré B., Platt SM, Silyakova A., Hermansen O., G. Allen, I. Pisso, Schmidbauer N., A. Stohl, Pitt J., P. Jansson, J. Greinert, Percival C. , Fjaeraa AM, O'Shea SJ, Gallagher M., Le Breton M., Bower KN, Bauguutte SJB, Dalsøren S., Vadakkepuliambatta S., Fisher RE, Nisbet EG, Lowry D., Myhre G., Pyle JA, M. Cain, J. Mienert Extensive release of methane from Arctic seabed west of Svalbard during summer 2014 not influence the does atmosphere // Geophysical Research Letters. 2016. Vol. 43 , pp. 4624 - 4631 .
 18. M. Saunio, of P. Bousquet, B. Poulter, A. The peregon of The global methane budget 2000-2012 // the System Earth Scientific the Data. 2016. Vol. 8. pp. 697-751.
 19. Shakhova N., Semiletov I., A. Salyuk, Yusupov V., D. Kosmach, Gustafsson O . Extensive methane venting to the atmosphere from sediments of the East Siberian Arctic Shelf // Science. 2010. Vol. 327. pp. 1246-1250.
 20. CA Varotsos, Tzanis the CG, the NV Sarlis the On the progress of the 2015-2016 El Niño event // the Atmospheric Chemistry and Physics. 2016. Vol. 16. pp. 2007-2011.

21. *M. Veloso, Greinert J., Mienert J., De Batist M.* A new methodology for quantifying bubble flow rates in deep water using splitbeam echosounders: Examples from the Arctic offshore NW-Svalbard // *Limnology Oceanography Methods* . 2015. Vol. 13. pp. 267-287.
22. *X. Xiong, C. Barnet, Maddy E., Gambacorta A., T. King, S. Wofsy* Mid-upper tropospheric methane retrieval from its validation IASI and // *Atmospheric Measurement Techniques*. 2013. Vol. 6: pp. 2255-2265.

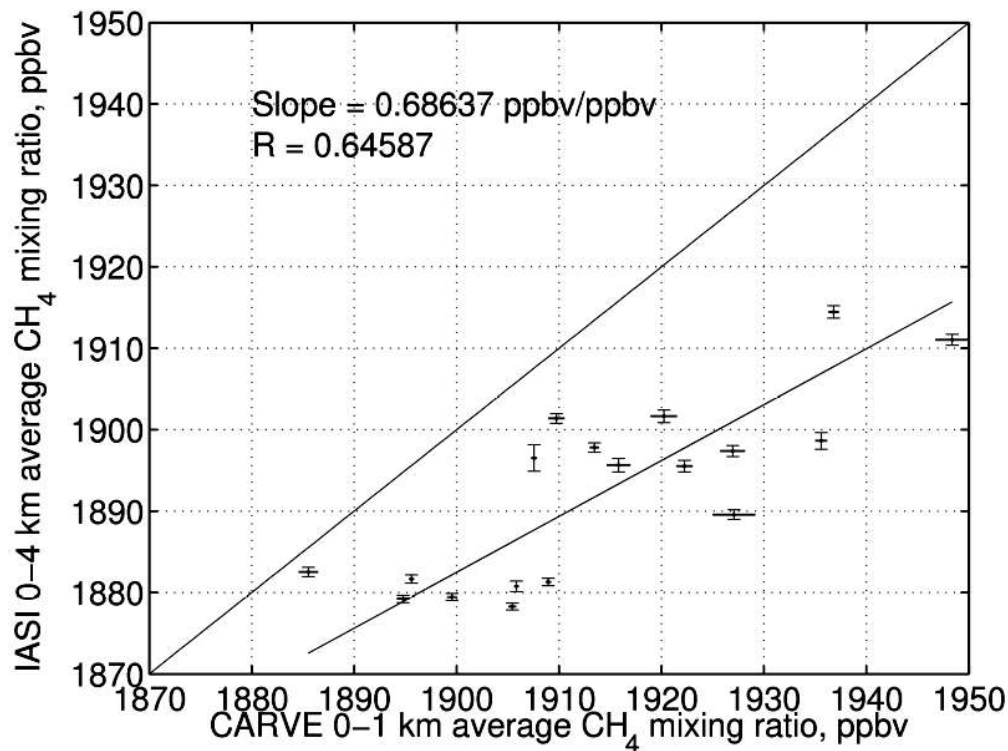


Fig. 1. Comparison of remote and airborne CH₄ Alaska data. The mean monthly methane concentrations measured by IASI over the southwestern part of Alaska are plotted versus direct measurements during the CARVE experiment. Vertical and horizontal bars correspond to $2 \text{ std } (N-1)^{-1/2}$, where std is the standard deviation of individual measurements and N is their number.

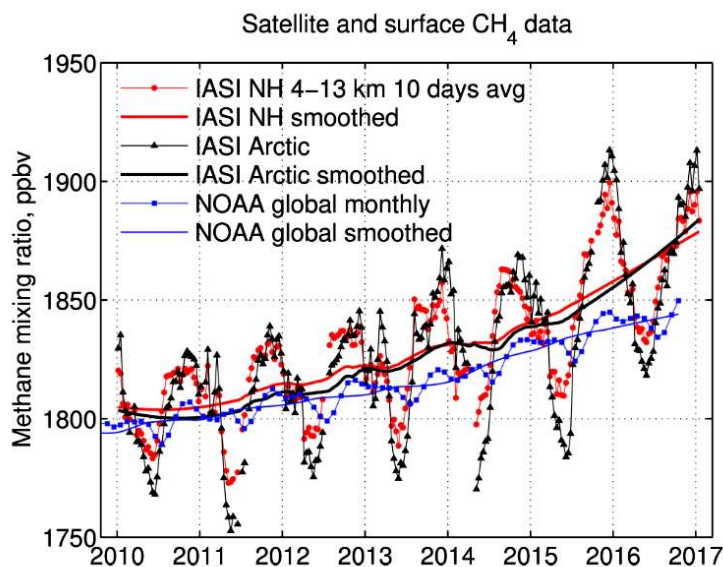


Fig. 2. Zonal average of methane concentrations above 4 km of altitude according to IASI (red circles for 45° N to 85° N and black triangles for 60° N to 85° N, respectively), in comparison with global ground-based measurements at the NOAA network (blue squares).

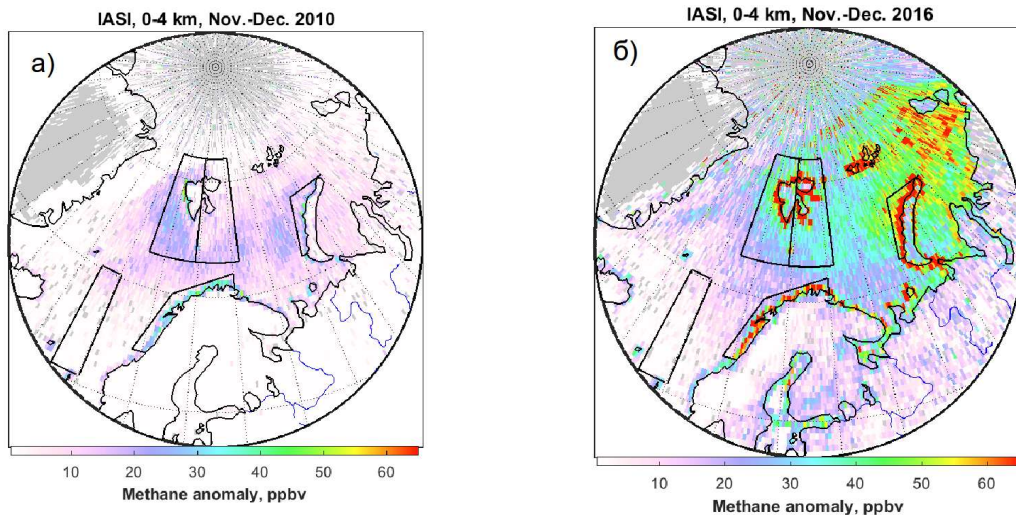


Fig. 3. a) Measured by IASI, averaged for November-December 2010 anomalies of methane concentration in the 0-4 km layer and gridded for $0.5^\circ \times 0.5^\circ$. b) The same for November-December 2016. An area between Scandinavia and Iceland is used as a reference.

IASI CH_4 anomaly for W. and E. of Svalbard, Nov.–Dec., 2010–2016

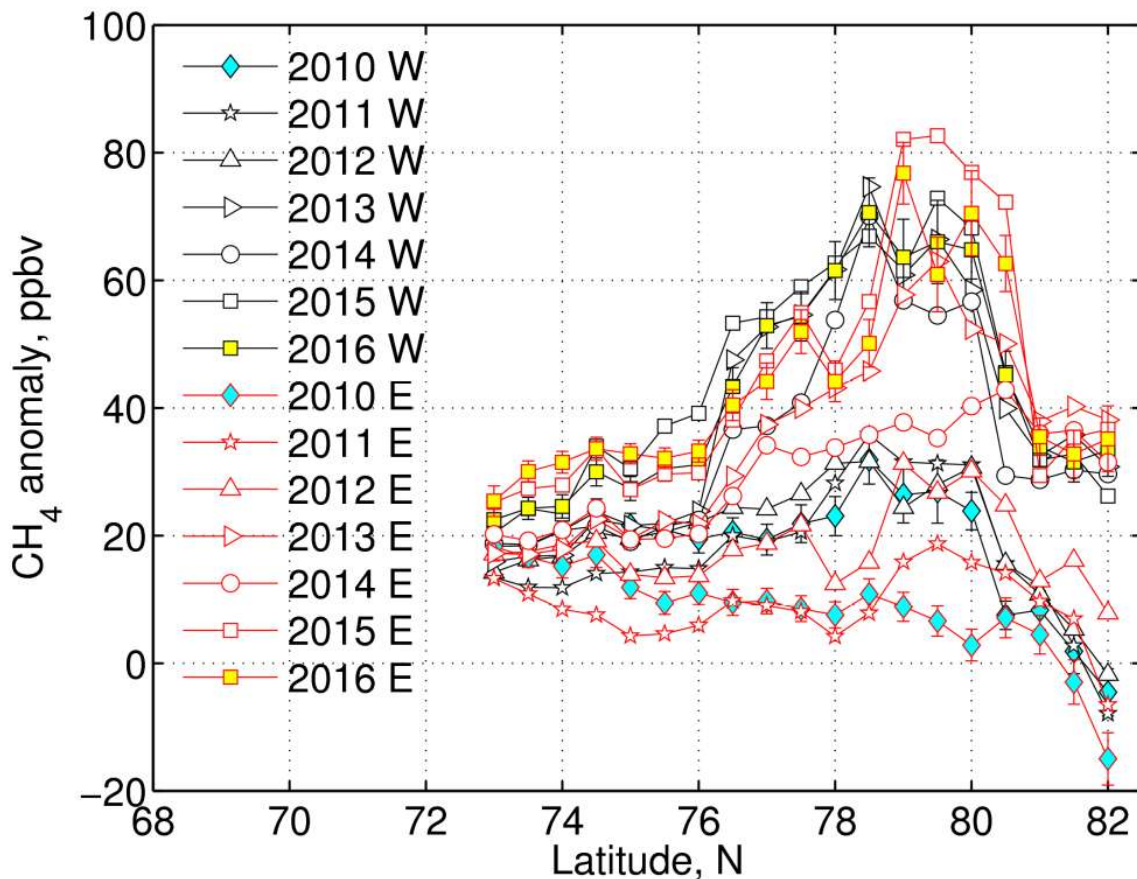


Fig. 4. The latitudinal dependence of the methane concentration anomaly for the two regions is to the West (black) and to the East of Svalbard (red). Vertical bars show the doubled mean square deviations for the mean. The boundaries of the regions are shown in Fig. 3.

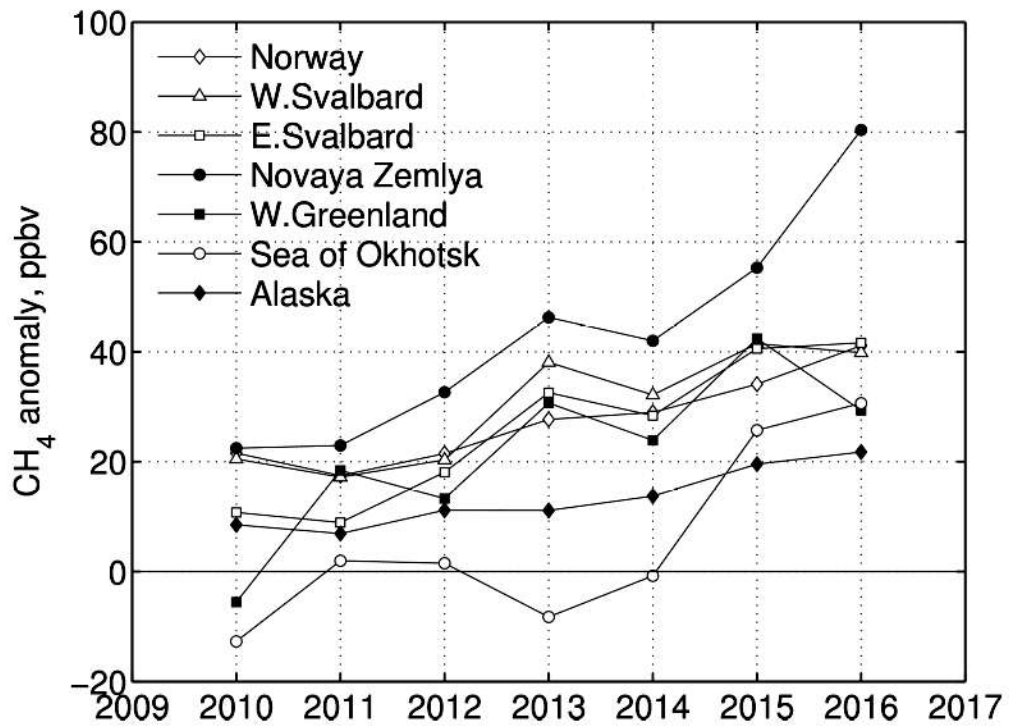


Fig. 5. Average anomalies of methane concentration in the autumn-winter period (November-December) for 5 regions of the seas of the Arctic Ocean and the Sea of Okhotsk. Summer-autumn data (for July-September) for the South-Western region of Alaska are also shown.

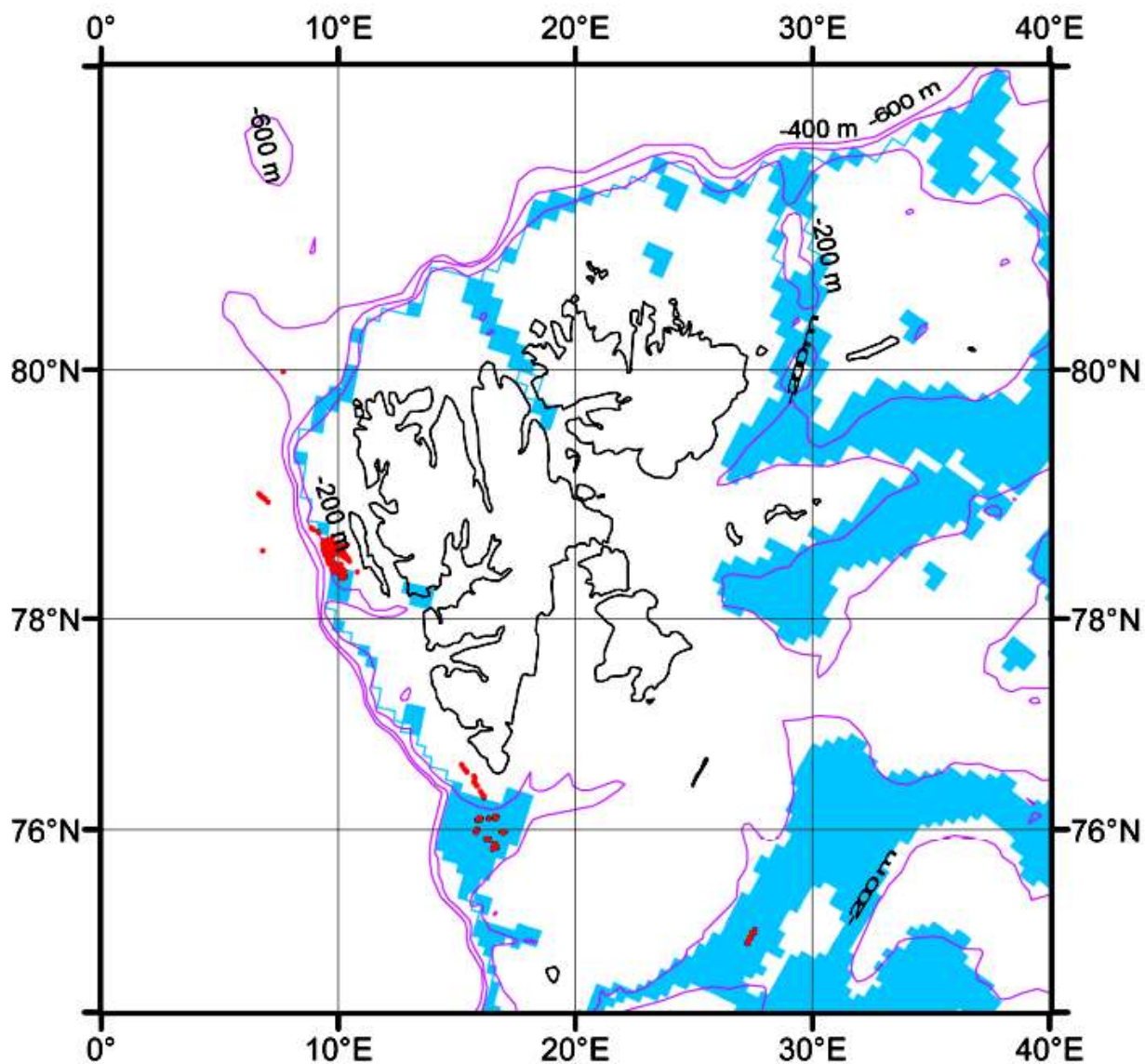


Fig. 6. Discovered to the West of Svalbard and shown in red are the positions of methane seeps. Blue shows potential areas of methane emission calculated by modeling the stability of methane hydrates at a given increase of the bottom water temperature. Crimson color shows isobaths.